.

# NUMERICAL ERROR ANALYSIS OF A SPLITTING METHOD FOR THE RESOLUTION OF THE ANISOTROPIC SCHRÖDINGER EQUATION.

CLAUDIA NEGULESCU

Abstract. This paper deals with the numerical analysis of three finite difference methods for the resolution of an anisotropic, linear 2D time-dependent Schrödinger equation. The physical context corresponding to this problem is the description of the interaction between a heavy particle and a light one, with the objective of depicting the decoherence induced on a quantum system by the environment. The principle aim of the present work is to study the convergence of splitting methods, applied to this highly anisotropic problem. The present paper provides moreover a numerical analysis support for the more computational paper [5] and prepares the arguments for the introduction of more efficient multi-scale schemes [4].

## 1. Introduction

The objective of this paper is the numerical analysis of the two-particle time-dependent Schrödinger equation

$$\left\{\begin{array}{l} \mathbf{i}\partial_t\psi = -\frac{1}{\delta}\Delta_y\psi - \frac{1}{\epsilon}\Delta_x\psi + \frac{1}{\varepsilon}V(|x-y|)\ \chi_{[0,\varepsilon]}(t)\ \psi\,, \quad \text{for} \quad (x,y)\in\Omega\,,\ \ t\in(0,T) \\ \partial_x\psi(t,x,y) = 0 \quad \text{on} \quad \partial\Omega_x\times\Omega_y\,; \qquad \partial_y\psi(t,x,y) = 0 \quad \text{on} \quad \Omega_x\times\partial\Omega_y \\ \psi(0,x,y) = \psi_0(x,y)\,, \quad \text{for} \quad (x,y)\in\Omega\,, \end{array}\right. \tag{1.1}$$

where the domain considered is $\Omega := \Omega_x\times\Omega_y = (0,1)\times(0,1)$ and $T$ is the final time considered. This equation describes the dynamics of a quantum system composed of a heavy and a light particle, interacting during the short time-interval $[0,\varepsilon]$ via a positive and regular potential $\frac{1}{\varepsilon}V(|x-y|)$ (repulsive interaction). Here $\psi(t,x,y)$ denotes the two-particle wave function, the quantity $|\psi(t,x,y)|^2dxdy$ representing the probability of finding at time $t$ the light particle (with mass $0<\varepsilon\ll 1$) in the volume $dx$ around the position $x$ and the heavy particle (with mass $\delta\sim\mathcal{O}(1)$) in the volume $dy$ around $y$. The Planck constant is normalized to one, by scaling, as we are not considering the semi-classical limit $\hbar\to 0$.

*Date*: January 25, 2012.

*Key words and phrases.* Quantum mechanics, Schrödinger equation, Heavy-light particle scattering, Interference, Decoherence, Numerical discretization, Numerical analysis, Splitting methods.

The aim of this paper is to study from a numerical analysis point of view (error estimates, convergence) three different finite difference schemes for the resolution of the highly anisotropic problem (1.1). The numerical resolution of this problem is rather delicate due to the presence of multiple scales in the dynamics, introduced by the small parameter $0 < \varepsilon \ll 1$. A detailed convergence study of the numerical schemes used, taking into account for the high anisotropies, is rather arduous and to the author's knowledge infrequent in the literature. The author proposes thus some insights in this direction and throughout the paper points out the numerical problems encountered. It is to be thought of as an indispensable support for the numerical results presented in the more computational paper [5]. Moreover, based on the conclusions one obtains, in particular on the rather pessimistic $\varepsilon$-dependent error estimates, a new performant scheme will be proposed in the forthcoming work [4], making use of multi-scale resolution techniques. Let us comment on all this in more details.

1.1. **Physical motivation.** For a more detailed physical interpretation of problem (1.1) we refer the interested reader to the articles [2, 3, 5], where the dynamics of this non-relativistic quantum-system are studied with the aim of understanding the so-called decoherence effect.
Briefly, quantum decoherence is judged to be the main reason for the emergence of classical behavior in a physical system, which is normally correctly described by quantum mechanics. The most important features of the quantum world are the superposition principle and entanglement. The observable characteristic of a quantum mechanical superposition state is the occurrence of interference fringes in the probability density associated to the state. However, the quantum coherence present in the unaffected superposition state is very fragile, and even a weak interaction with the environment can destroy the interference pattern, in particular destroying the phase relations between the different states in the superposition, and a classical behavior of the system emerges. This reduction or even suppression of the interference fringes in a quantum system, induced by the environment, is called decoherence effect.
It is important to remark here that decoherence is different from the semi-classical procedure $\hbar \to 0$, as it acts on the scale of the interference fringes. Moreover, understanding this phenomenon is crucial not only for quantum computation, where it is not desired, but also for the design of new semiconductor devices, such as the QuIET.

The objective of the toy-model we conceive, is to study numerically the mechanism of decoherence in the simplest model in which it takes place, where a heavy particle (for example oxygen ion or proton) scatters a light one (for example electron or positron). The two particles interact via a repulsive potential and, due to the low mass-ratio, the light

particle is scattered while the heavy particle remains almost unperturbed. It turns out that, at leading order in the mass ratio, the only effect of the interaction on the heavy particle is the destruction of the interference pattern. It is important to mention that the small mass ratio is crucial in order to single out the decoherence effect and to neglect effects like deformation and energy exchange between the particles.

To facilitate the comprehension of the meaning of decoherence, the author plotted in Figure 1 the heavy particle density function $\rho_H(t,y)$ (for two different time-instants $t$), defined by

$$\rho_H(t,y) := \int_{-\infty}^{\infty} |\psi(t,x,y)|^2 \, dx \,, \quad t \in [0,T] \,. \tag{1.2}$$

This simulation is performed, starting with the initial condition

$$\psi(0,x,y) = \left(\varphi_0(y-y_0)\, e^{\frac{-\mathrm{i}P_H y}{\hbar}} + \varphi_0(y+y_0)\, e^{\frac{\mathrm{i}P_H y}{\hbar}}\right) \chi_0(x) \,, \tag{1.3}$$

which represents two particles being at time zero completely uncorrelated. The two functions $\varphi_0$ and $\chi_0$ are Gaussian wave packets

$$\varphi_0(y) := \frac{\beta}{(2\pi)^{1/4}\sqrt{\sigma_H}} e^{-\frac{y^2}{4\sigma_H^2}} \,, \quad \chi_0(x) := \frac{1}{(2\pi)^{1/4}\sqrt{\sigma_L}} e^{-\frac{(x-x_0)^2}{4\sigma_L^2}} e^{\frac{-\mathrm{i}P_L x}{\hbar}} \,, \tag{1.4}$$

with $\beta \in \mathbb{R}^+$ chosen so that the initial condition satisfies $\|\psi_0\|_{L^2(\Omega)} = 1$. Let us remark that the heavy particle is given initially in the form of two bumps moving towards each other (see left figure), the plot on the right corresponding to the instant $\overline{t} := \frac{y_0 \delta}{P_H}$, where the two heavy-particle wave-packets completely overlap. Three different curves are plotted, corresponding to the fully quantum mechanical superposition picture (when no interaction between the heavy and the light particle is present), the fully classical picture (a simple summation of the two bumps) and the partially decoherent picture. The effect of decoherence is thus the reduction of the interference pattern, and this due to the loss of phase relations between the different superposition states.

Let us mention that the quantum system (1.1) appears also in other physical/chemical/ biological contexts, for example in the modeling of the dynamics of molecular systems, composed of heavy nuclei and light electrons, describing the interaction processes between these constitutive elements.

1.2. **Numerical difficulties and aim of this paper.** Let us comment now a little on the numerical difficulties encountered when trying to solve system (1.1) and let us briefly introduce the different schemes investigated in this paper.

For more clarity, the author would like to observe firstly, that the physical problem is posed in general in the whole of $\mathbb{R}^2$ space. However, for the calculations, bounded domains

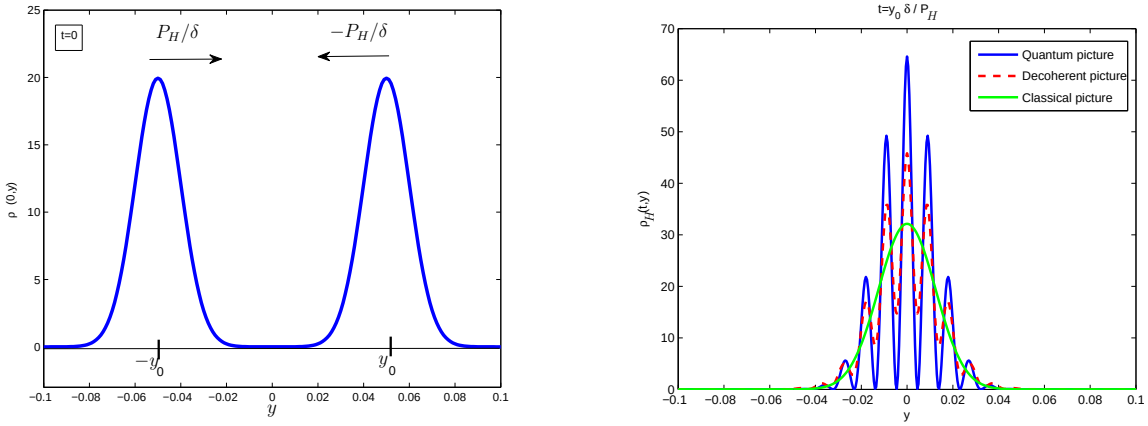


FIGURE 1. Left: Initially, the heavy particle is given under the form of two wave-packets moving against each other. Here is plotted the corresponding probability density. Right: Partially decoherent superposition of the two heavy particle bumps, at overlap time $\bar{t}$.

are required and thus adequate boundary conditions. In the primary work [5] homogeneous Neumann boundary conditions are chosen to simplify the numerical simulation of the 2D Schrödinger equation and to concentrate on the study of the decoherence effect. The two particles are thus reflected when touching the boundary, constituting in this manner a sort of *quantum pendulum*. However, the thus induced permanent presence of both particles in the domain, imposes truncation of the interaction potential $V$ after an interaction time of the order $\mathcal{O}(\varepsilon)$, in order to correctly describe the physics. Note that in the whole $\mathbb{R}^2$-space dynamics, the efficient interaction between the two particles persists over a period proportional to $\varepsilon$ and this due to the rapid dispersion of the light particle. This fact provides an "explanation" of the potential-truncation procedure used here. Artificial (or absorbing) boundary conditions would make this truncation unnecessary, however they would complicate considerably the numerical resolution and are not even needed if one considers a single heavy-light collision.

The numerical resolution of system (1.1) poses extremely challenging problems. It is an example of a multi-scale problem, due to the small parameter $0 < \varepsilon \ll 1$. The light particle has a rapid dynamics (rapid dispersion), whereas the heavy one responds on relatively long time scales. The decoherence effect, which is the phenomenon we want to study, appears clearly in the limit $\varepsilon \to 0$, as explained in detail in [3]. For very large $\varepsilon$-values, deformation-effects eclipse the desired decoherence effect. However, very small $\varepsilon$-values lead to sever numerical problems, as shall be seen in this paper. We are thus in a sort of dilemma: On the one hand, for large $\varepsilon$-values we have precise, but uninteresting

results (with deformation) and on the other hand, very interesting decoherence results can be studied for $0 < \varepsilon \ll 1$, but a lot of work and attention is needed to avoid numerical difficulties and to get precise results. The objective here shall be to analyze three numerical methods for the "delicate" resolution of (1.1) in the small $\varepsilon$-regime, and to give the error estimates necessary to validate the numerical computations presented in [5].

For the short presentation of the three methods, we shall firstly forget about the potential truncation. One possible way to solve (1.1) would be to use the Crank-Nicolson scheme. Writing the 2D Schrödinger equation (1.1) in the form

$$\begin{cases} \partial_t \psi = \mathbf{i} G\psi \,, \quad \text{on } (0,T)\,, \\ \psi(t=0) = \psi_0 \,, \end{cases}$$

where $G$ is the unbounded operator

$$G : D(G) \subset X \to X \,, \quad G\psi := \frac{1}{\delta}\Delta_y \psi + \frac{1}{\varepsilon}\Delta_x \psi - \frac{1}{\varepsilon} V\psi \,,$$

with $X := L^2(\Omega)$ and definition domain $D(G) \subset X$, the Crank-Nicolson scheme writes

$$\frac{\psi^{n+1} - \psi^n}{\Delta t} = \mathbf{i} G \, \frac{\psi^{n+1} + \psi^n}{2} \,,$$

which can also be written as

$$\psi^{n+1} = (I - \mathbf{i}\frac{\Delta t}{2} G)^{-1} (I + \mathbf{i}\frac{\Delta t}{2} G)\, \psi^n \,, \quad \forall n \in \mathbb{N}\,.$$

Here $\Delta t > 0$ denotes the discretization time-step. This method is unconditionally stable and second order accurate in time, thus making it very attractive. However, there are some rather servere disadvantages, which will force us to choose an alternative scheme.
Firstly, due to the small parameter $0 < \varepsilon \ll 1$, the time step has to be chosen very small in order to resolve the small time-scales (or catch the rapid dynamics) and to obtain accurate results, which means that many time iteration-steps $n$ have to be performed. Secondly, at each time-step $n$, a linear system corresponding to a 2D problem has to be solved (the scheme being implicit). As the small parameter $\varepsilon$ intercedes also in the space scales, forcing us to choose a fine grid in the $x$- and $y$-directions, the linear system to be solved at each time-step $n$ shall be huge and ill-conditioned, resulting consequently in prohibitively expensive computations.

These disadvantages lead us to use splitting methods, which consist in solving several 1D Schrödinger-type systems instead of the 2D system (1.1), and permit thus considerable computational time and memory savings. For this, the 2D operator $G$ shall be split into

$G := A + B$, with the unbounded operator $A$

$$A : D(A) \subset X \to X\,, \quad A\psi := \frac{1}{\delta}\Delta_y\psi\,, \quad \overline{A} := \delta A\,,$$

and the stiff, unbounded operator $B$

$$B : D(B) \subset X \to X\,, \quad B\psi := \frac{1}{\varepsilon}\Delta_x\psi - \frac{1}{\varepsilon}V\psi\,, \quad \overline{B} := \varepsilon B\,.$$

We shall now solve the Schrödinger equation either by the Lie splitting scheme

$$\psi^{n+1} = (I - \mathbf{i}\Delta t B)^{-1}(I - \mathbf{i}\Delta t A)^{-1}\,\psi^n\,,$$

which is an unconditionally stable, first order (in time) scheme, or the Peaceman-Rachford splitting scheme

$$\psi^{n+1} = (I - \mathbf{i}\frac{\Delta t}{2}B)^{-1}(I + \mathbf{i}\frac{\Delta t}{2}A)(I - \mathbf{i}\frac{\Delta t}{2}A)^{-1}(I + \mathbf{i}\frac{\Delta t}{2}B)\,\psi^n\,,$$

which is unconditionally stable with respect to the $L^2$-norm and second order in time. By decomposing the initial 2D Schrödinger problem into two 1D sub-problems, we firstly significantly accelerate the numerical resolution of (1.1). On the other hand, a second and to the author's opinion essential advantage is that the splitting procedure somehow separates the two appearing scales (even if they remain coupled), which will permit a different numerical treatment of the two sub-problems and also the introduction of efficient numerical algorithms for the stiff sub-problem. This idea shall be persued in future work.

The aim of this paper is to analyze from a numerical point of view these two splitting methods as well as the Crank-Nicolson scheme, in particular to study their convergence and to estimate their errors, with some special regard to the $\varepsilon$-dependence. Moreover we shall weigh the obtained numerical results in comparing the computational times as well as the numerical precisions. Several papers in the literature are concerned with splitting methods. A non-exhaustive list is [6–12, 14, 15, 18], as well as the references therein. However, in the author's opinion, no work treats highly anisotropic, oscillating problems, like the one which is the starting point of the present paper. It would be interesting to understand how the errors depend on the anisotropy parameter $\varepsilon$, and what has to be done, to avoid the problematic, time and memory demanding choice of very fine time and space discretization meshes. The arguments used to cope with this new problem, follow at times the arguments of all the works cited previously.

Apart the fact that the present numerical analysis gives some interesting insights into the (very painful) numerical study of schemes used for the discretization of highly anisotropic problems, it is also very important as a support for the numerical results presented in [5], with the aim of describing the "delicate" decoherence effect. On the other hand, based on

this numerical analysis and its conclusions, performant numerical schemes shall be introduced in the future work [4], better suited to the challenging resolution of the multi-scale problem (1.1). In the last part of this paper, the author presents the basic ideas for the construction of such a multi-scale scheme, founded on the study of the asymptotic behavior of the wave-function $\psi(t,x,y)$ in the limit $\varepsilon \to 0$. The main idea is essentially the separation of the two heavy-light dynamics.

The structure of this paper is the following. In Section 2, the mathematical framework of this work is specified and the different numerical schemes are presented. Section 3 is concerned with the numerical analysis of these schemes. Error estimates are proved and conclusions are deduced for the applications investigated in [5]. Finally, in Section 4 the foundation is prepared for a more performant multi-scale scheme.

## 2. Mathematical framework and introduction of the numerical schemes

In this section, we introduce the mathematical framework needed for the numerical analysis of the Crank-Nicolson method as well as the Lie and Peaceman-Rachford splitting methods, used for the resolution of the 2D Schrödinger equation (1.1).

### 2.1. **Functional spaces and operators.**

The operators introduced here and their properties shall be used throughout this paper. Recall that $\Omega := \Omega_x \times \Omega_y = (0,1) \times (0,1)$ and $T > 0$ is a given final time. Recall moreover, that during the time-interval $[0, \varepsilon]$ we have an interaction potential $V \neq 0$, whereas afterwards, during $[\varepsilon, T]$, there is no more interaction and we can put $V \equiv 0$. In the following let $X := L^2(\Omega)$ be the complex Hilbert space, associated with the standard scalar product

$$(\phi, \theta) := \int_\Omega \phi\, \overline{\theta}\, dxdy\,, \quad \forall \phi, \theta \in X\,.$$

Now define the following unbounded operators $G := A + B$

$$G : D(G) \subset X \to X\,, \quad G\psi := \frac{1}{\delta}\Delta_y \psi + \frac{1}{\varepsilon}\Delta_x \psi - \frac{1}{\varepsilon} V\psi\,,$$

$$A : D(A) \subset X \to X\,, \quad A\psi := \frac{1}{\delta}\Delta_y \psi\,; \quad B : D(B) \subset X \to X\,, \quad B\psi := \frac{1}{\varepsilon}\Delta_x \psi - \frac{1}{\varepsilon} V\psi\,,$$

where, for more clarity, we shall denote sometimes in the sequel by $G_0$ resp. $B_0$ the operators $G$ resp. $B$ corresponding to the special free motion case $V \equiv 0$. The potential $V$ is supposed regular and repulsive, i.e. $V \in C^\infty(\overline{\Omega})$ and $V \geq 0$. The definition domains of these operators are given by

$$
\begin{aligned}
D(G) &:= \{\psi \in H^1(\Omega) \,/\, \Delta\psi \in L^2(\Omega)\,, \partial_n\psi = 0 \text{ on } \partial\Omega\} \subset H^2(\Omega)\,,\\
D(A) &:= \{\psi \in L^2(\Omega) \,/\, \partial_y\psi \in L^2(\Omega)\,, \partial^2_{yy}\psi \in L^2(\Omega)\,, \partial_y\psi = 0 \text{ on } \Omega_x \times \partial\Omega_y\}\,,\\
D(B) &:= \{\psi \in L^2(\Omega) \,/\, \partial_x\psi \in L^2(\Omega)\,, \partial^2_{xx}\psi \in L^2(\Omega)\,, \partial_x\psi = 0 \text{ on } \partial\Omega_x \times \Omega_y\}\,,
\end{aligned}
$$

where $\partial_n$ denotes the outward normal to the boundary $\partial\Omega$.
The thus defined unbounded operators $G$, $A$ and $B$ are self-adjoint. Indeed, they are symmetric and the property of the range $R(F \pm \mathbf{i}I) = X$ is satisfied, where $F$ shall denote in the sequel one of the operators $G$, $A$ or $B$ and where $I$ stands for the identity operator. Stone's theorem [16] implies that

$$
\tilde{G} := \mathbf{i}G\,, \quad \tilde{A} := \mathbf{i}A\,, \quad \tilde{B} := \mathbf{i}B\,,
$$

are generators of unitary (semi-)groups, denoted by $\mathcal{G}(t) \in \mathcal{L}(X)$, $\mathcal{A}(t) \in \mathcal{L}(X)$ resp. $\mathcal{B}(t) \in \mathcal{L}(X)$.
Moreover, as $G$, $A$ and $B$ are self-adjoint, one deduces that the resolvants $\rho(\tilde{G})$, $\rho(\tilde{A})$ and $\rho(\tilde{B})$ contain $\mathbb{R}^*$, implying the existence of the following inverse operators and their bounds:

$$
||(I - \Delta t\tilde{G})^{-1}||_{\mathcal{L}(X)} \leq 1\,, \quad ||(I - \Delta t\tilde{A})^{-1}||_{\mathcal{L}(X)} \leq 1\,, \quad ||(I - \Delta t\tilde{B})^{-1}||_{\mathcal{L}(X)} \leq 1\,, \quad \forall \Delta t \in \mathbb{R}\,.
$$

Notice also that $R((I - \Delta t\tilde{F})^{-1}) = D(F)$, for all $\Delta t \in \mathbb{R}$. Furthermore remark that these operators are conservative, which means

$$
\mathcal{R}e(\tilde{F}\psi, \psi)_X = 0\,, \quad \forall \psi \in D(F)\,.
$$

This property allows one to show that

$$
||(I - \Delta t\tilde{F})^{-1}(I + \Delta t\tilde{F})||_{\mathcal{L}(X)} = 1\,, \quad \text{for all} \quad \Delta t \in \mathbb{R}\,.
$$

With these notations one can now rewrite the 2D Schrödinger equation (1.1) in the following evolution form

$$
\left\{ \begin{array}{l} \partial_t\psi^{(1)} = \tilde{G}\psi^{(1)}\,, \quad \text{on} \quad (0, \varepsilon) \\ \psi^{(1)}(t = 0) = \psi_0\,, \quad \psi_0 \in D(G) \end{array} \right. , \qquad \left\{ \begin{array}{l} \partial_t\psi^{(2)} = \tilde{G}_0\psi^{(2)}\,, \quad \text{on} \quad (\varepsilon, T) \\ \psi^{(2)}(t = \varepsilon) = \psi^{(1)}(\varepsilon)\,. \end{array} \right. \tag{2.5}
$$

Is is now a simple consequence that system (2.5) admits a unique solution, which can be written as

$$
\psi^{(1)}(t) = \mathcal{G}(t)\psi_0\,, \quad \forall t \in [0, \varepsilon]\,, \quad \psi^{(2)}(t) = \mathcal{G}_0(t - \varepsilon)\psi^{(1)}(\varepsilon)\,, \quad \forall t \in [\varepsilon, T]\,. \tag{2.6}
$$

The semi-group theory [16] allows us to prove the following properties of this exact solution.

**Proposition 2.1.** *Let $\tilde{G}$ be the unbounded operator defined above and generator of the unitary, conservative semi-group $\mathcal{G}(t) \in \mathcal{L}(X)$ and let $\psi_0 \in D(G)$. Then the Cauchy problem*

*(2.5) admits a unique solution $\psi$, given by (2.6) and satisfying*

*(i)* $\psi(t) \in D(G),\ \forall t \geq 0$,
*(ii)* $\psi \in C^0([0,T];X) \cap C^1((0,\varepsilon);X) \cap C^1((\varepsilon,T);X)$,
*(iii) Conservation of the probability density*

$$||\psi(t)||_X = ||\psi_0||_X\,, \quad \forall t \geq 0\,,$$

*(iv) Conservation of the energy*

$$||\psi(t)||^2_{\mathcal{H}} := \frac{1}{\delta}||\partial_y\psi(t)||^2_X + \frac{1}{\varepsilon}||\partial_x\psi(t)||^2_X + \frac{1}{\varepsilon}||\sqrt{V}\psi(t)||^2_X = ||\psi_0||^2_{\mathcal{H}}\,, \quad \forall t \in [0,\varepsilon]\,,$$

$$||\partial_x\psi(t)||_X = ||\partial_x\psi(\varepsilon)||_X\,, \quad ||\partial_y\psi(t)||_X = ||\partial_y\psi(\varepsilon)||_X\,, \quad \forall t \in [\varepsilon,T]\,,$$

*(v) If $\psi_0 \in D(G^l)$ for some $l \in \mathbb{N}$, then we have the conservation*

$$||\tilde{G}^k\psi(t)||_X = ||\tilde{G}^k\psi_0||_X\,, \quad \forall t \in [0,\varepsilon]\,, \quad ||D^\alpha\psi(t)||_X = ||D^\alpha\psi(\varepsilon)||_X\,, \quad \forall t \in [\varepsilon,T]\,,$$

*with $0 \leq k \leq l$ and $\alpha \in \mathbb{N}^2$ such that $|\alpha| := \alpha_1 + \alpha_2 \leq 2l$, the $\alpha$th order derivative being given as $D^\alpha = \frac{\partial^{|\alpha|}}{\partial_x^{\alpha_1}\partial_y^{\alpha_2}}$.*

**Proof:** We shall not prove here this theorem, which is a simple consequence of the semi-group theory. We want only to remark that the conservation

$$||D^\alpha\mathcal{G}_0(t-\varepsilon)\psi(\varepsilon)||_X = ||D^\alpha\psi(t)||_X = ||D^\alpha\psi(\varepsilon)||_X = ||\mathcal{G}_0(t-\varepsilon)D^\alpha\psi(\varepsilon)||_X\,, \tag{2.7}$$

in the free-motion interval $t \in [\varepsilon,T]$ follows by standard arguments, for example multiplying the free-motion Schrödinger equation by a suitable derivative of $\psi$ ($\psi$, $\partial_x\psi$, $\partial_y\psi$, etc.), integrating by parts and taking the real or imaginary part. ∎

2.2. **Numerical schemes.** Formula (2.6) gives the exact solution of our evolution problem (2.5), however it is an abstract form, which does not permit the computation of $\psi(t)$. We shall thus turn our attention to numerical methods.

To solve (2.5) by means of the Crank-Nicolson scheme, we introduce the homogeneous discretization of the time interval $[0,T]$

$$0 = t_0 \leq \cdots \leq t_n \leq \cdots \leq t_K = T\,, \quad \text{where} \quad \Delta t := t_{n+1} - t_n > 0\,,$$

where we insist that for some index $n_0 \in \mathbb{N}$ we have $t_{n_0} = \varepsilon$. Then the Crank-Nicolson scheme gives

$$\frac{\psi^{n+1}_{CN} - \psi^n_{CN}}{\Delta t} = \tilde{G}\,\frac{\psi^{n+1}_{CN} + \psi^n_{CN}}{2}\,,$$

which can also be written, with the unitary Crank-Nicolson operator $C^K(t) \in \mathcal{L}(X)$, as

$$\psi^{n+1}_{CN} = C^K(\Delta t)\psi^n_{CN} := (I - \frac{\Delta t}{2}\tilde{G})^{-1}(I + \frac{\Delta t}{2}\tilde{G})\,\psi^n_{CN}\,, \quad \forall n \in \mathbb{N}\,. \tag{2.8}$$

The notation $\psi_{CN}^n \in D(G)$ stands for the time-approximation at $t_n$ of the exact solution $\psi(t_n) \in D(G)$ via the Crank-Nicolson scheme. Remark that, for simplicity, we shall always denote in the sequel, there where no confusion can occur, $\tilde{G}$ resp. $\tilde{B}$ even for $\tilde{G}_0$ resp. $\tilde{B}_0$. Remember however, that for $n \geq n_0$ the corresponding operators reduce to $\tilde{G}_0$ resp. $\tilde{B}_0$.

Let us now introduce the splitting methods for the resolution of system (2.5). In the following $\psi_{spl}(t_n)$ shall denote the splitting approximation of $\psi(t_n) \in D(G)$. The basic idea of the splitting methods presented here is to treat the two directions separately. The Lie splitting method consists in advancing first a time step in the $y$ direction and then another time step in the $x$ direction. This gives

$$\left\{ \begin{array}{l} \partial_t \psi_1 = \tilde{A}\psi_1 \,, \quad \text{on} \quad (t_n, t_{n+1}) \\ \psi_1(t_n) = \psi_{spl}(t_n) \end{array} \right. ; \left\{ \begin{array}{l} \partial_t \psi_2 = \tilde{B}\psi_2 \,, \quad \text{on} \quad (t_n, t_{n+1}) \\ \psi_2(t_n) = \psi_1(t_{n+1}) \,. \end{array} \right. , \tag{2.9}$$

$$\psi_{spl}(t_{n+1}) := \psi_2(t_{n+1}) \,,$$

where one starts with $\psi_{spl}(t_0) := \psi_0$. Knowing that $\tilde{A}$ and $\tilde{B}$ generate the semi-groups $\mathcal{A}(t)$ resp. $\mathcal{B}(t)$, we can write the exact splitting solution of (2.9) as

$$\psi_{spl}(t_{n+1}) = \mathcal{L}(\Delta t)\psi_{spl}(t_n) \,, \quad \text{where } \mathcal{L}(\Delta t) := \mathcal{B}(\Delta t)\mathcal{A}(\Delta t) \,, \quad \forall n \in \mathbb{N} \,.$$

The unitary operator $\mathcal{L}(\Delta t) \in \mathcal{L}(X)$ is the Lie-operator.
The Strang splitting method consists of three steps.

$$\left\{ \begin{array}{l} \partial_t \psi_1 = \tilde{B}\psi_1 \,, \quad \text{on} \quad (t_n, t_{n+1/2}) \\ \psi_1(t_n) = \psi_{spl}(t_n) \end{array} \right. ; \left\{ \begin{array}{l} \partial_t \psi_2 = \tilde{A}\psi_2 \,, \quad \text{on} \quad (t_n, t_{n+1}) \\ \psi_2(t_n) = \psi_1(t_{n+1/2}) \,, \end{array} \right. , \tag{2.10}$$

$$\left\{ \begin{array}{l} \partial_t \psi_3 = \tilde{B}\psi_3 \,, \quad \text{on} \quad (t_{n+1/2}, t_{n+1}) \\ \psi_3(t_{n+1/2}) = \psi_2(t_{n+1}) \end{array} \right. ; \quad \psi_{spl}(t_{n+1}) := \psi_3(t_{n+1}) \,, \tag{2.11}$$

where again $\psi_{spl}(t_0) := \psi_0$. The exact split solution writes

$$\psi_{spl}(t_{n+1}) = \mathcal{S}(\Delta t)\psi_{spl}(t_n) \,, \quad \text{where } \mathcal{S}(\Delta t) := \mathcal{B}(\frac{\Delta t}{2})\mathcal{A}(\Delta t)\mathcal{B}(\frac{\Delta t}{2}) \,, \quad \forall n \in \mathbb{N} \,.$$

The unitary operator $\mathcal{S}(\Delta t) \in \mathcal{L}(X)$ is the Strang-operator.

It is however impossible to compute the semi-groups $\mathcal{A}(t)$ and $\mathcal{B}(t)$, and thus the Lie and Strang operators. Consequently, we shall discretize them in time. Choosing the implicit Euler scheme for both systems in (2.9) leads to the semi-discretized (in time) Lie-scheme

$$\psi_{spl}^{n+1} = L^K(\Delta t)\psi_{spl}^n := (I - \Delta t\tilde{B})^{-1}(I - \Delta t\tilde{A})^{-1}\psi_{spl}^n \,, \tag{2.12}$$

where $\psi_{spl}^n$ denotes the approximation of the splitting solution $\psi_{spl}(t_n)$ and where $\psi_{spl}^0 := \psi_0$. Now the operator $L^K(\Delta t) \in \mathcal{L}(X)$ is no longer unitary, but only contractive.
Choosing the Euler explicit method for the first system in (2.10), the Euler implicit method

for the second system on $(t_n, t_{n+1/2})$ only and then the Euler explicit for the remainder of the interval $(t_{n+1/2}, t_{n+1})$, and finally the Euler implicit method for the third system (2.11), gives rise to the Peaceman-Rachford-scheme

$$\psi_{spl}^{n+1} = P^K(\Delta t)\psi_{spl}^n := (I - \frac{\Delta t}{2}\tilde{B})^{-1}(I + \frac{\Delta t}{2}\tilde{A})(I - \frac{\Delta t}{2}\tilde{A})^{-1}(I + \frac{\Delta t}{2}\tilde{B})\psi_{spl}^n \,. \qquad (2.13)$$

The Crank-Nicolson, Lie and Peaceman-Rachford schemes are well defined, by the remarks of Section 2.1. Remark that, while the Crank-Nicolson and Lie schemes are stable, the linear Peaceman-Rachford operator $P^K(\Delta t) : D(B) \to D(B)$ satisfies only

$$||P^K(\Delta t)\psi||_X \leq ||(I + \frac{\Delta t}{2}\tilde{B})\psi||_X \,, \quad \forall \psi \in D(B) \,,$$

which means, that the scheme (2.13) is weakly stable. We refer to [17] for a detailed study. In the following, for simplicity, let $\mathcal{F}(t) \in \mathcal{L}(X)$ denote one of the splitting operators $\mathcal{L}(t)$ or $\mathcal{S}(t)$. Moreover let $F^K(\Delta t)$ stand for one of the semi-discretized splitting operators $L^K(\Delta t)$ or $P^K(\Delta t)$, or even the Crank-Nicolson operator $C^K(\Delta t)$, given in (2.8).

Up to this point, we have investigated only the splitting procedure and the time-discretization. Indeed, the schemes (2.8), (2.12) and (2.13) are three different time discretizations of the system (2.5). However, we also have to consider the spatial-discretization. First, we discretize in space $(x, y)$ the initial system (2.5) and then apply, as before, the operator splitting procedures and time-discretizations to the spatially semi-discretized system. This leads to the following steps:

1. Approximation of the continuous system (2.5) by a second-order spatial discretization scheme (semi-discretization in space) $\to$ system of ordinary differential equations.
2. For the splitting methods: Directional splitting of the space-discretized operator $\to$ two or three smaller systems of ordinary differential equations.
3. Approximation of the time-continuous systems by appropriate time-discretization methods (Euler implicit/Euler explicit/Crank-Nicolson for example) $\to$ fully numerical schemes (linear algebraic systems to be solved).

For this, let

$$0 = x_0 \leq \cdots \leq x_i \leq \cdots \leq x_{N+1} = 1 \,, \quad 0 = y_0 \leq \cdots \leq y_j \leq \cdots \leq y_{M+1} = 1 \,,$$

be a homogeneous discretization of the domain $\overline{\Omega}$, with the corresponding space steps $\Delta x > 0$ and $\Delta y > 0$. Associated with this discretization, we define the finite dimensional Hilbert space $X_{NM} := \mathbb{C}^{NM}$, with the scalar product

$$(u, v)_{X_{NM}} := \Delta x \Delta y \sum_{l=1}^{N \times M} u_l \, \overline{v_l} \,,$$

which shall approximate the infinite dimensional space $X = (L^2(\Omega), (\cdot,\cdot))$. Let us also introduce the linear and bounded projection operator $\mathcal{P}_{NM}$ between the original and the approximating space

$$\mathcal{P}_{NM} : X \to X_{NM}\,, \quad \psi \in X \longmapsto (\psi_{ij})_{i,j=1}^{N,M} := (\psi(x_i, y_j))_{i,j=1}^{N,M} \in X_{NM}\,. \tag{2.14}$$

Designating by $\tilde{B}_{NM} \in \mathbb{C}^{NM\times NM}$ the standard second order discretization of the operator $\tilde{B}$

$$\tilde{B}_{NM} := -\frac{\mathbf{i}}{\varepsilon(\Delta x)^2}\begin{pmatrix} T_1 & & \\ & \ddots & \\ & & T_M \end{pmatrix}, \quad \text{where}$$

$$T_j := \begin{pmatrix} 1+(\Delta x)^2 V_{1j} & -1 & & & & & \\ -1 & 2+(\Delta x)^2 V_{2j} & -1 & & & & \\ & & \ddots & & & & \\ & & & -1 & 2+(\Delta x)^2 V_{N-1,j} & -1 & \\ & & & & -1 & 1+(\Delta x)^2 V_{Nj} & \end{pmatrix},$$

by $\tilde{A}_{NM} \in \mathbb{C}^{NM\times NM}$ that of the operator $\tilde{A}$ and by $\tilde{G}_{NM} \in \mathbb{C}^{NM\times NM}$ that of $\tilde{G}$, these matrices are (similar to the continuous case) skew-adjoint and conservative, that means

$$\mathcal{R}e(\tilde{A}_{NM}u, u)_{X_{NM}} = 0\,, \quad \mathcal{R}e(\tilde{B}_{NM}u, u)_{X_{NM}} = 0\,, \quad \mathcal{R}e(\tilde{G}_{NM}u, u)_{X_{NM}} = 0\,, \quad \forall u \in \mathbb{C}^{NM}\,.$$

The associated unitary semi-groups are denoted by $\mathcal{A}_{NM}(t) \in \mathcal{L}(X_{NM})$, $\mathcal{B}_{NM}(t) \in \mathcal{L}(X_{NM})$ and $\mathcal{G}_{NM}(t) \in \mathcal{L}(X_{NM})$. Furthermore we have the properties

$$||(I - \Delta t\tilde{F}_{NM})^{-1}||_{\mathcal{L}(X_{NM})} \leq 1\,, \quad ||(I - \Delta t\tilde{F}_{NM})^{-1}(I + \Delta t\tilde{F}_{NM})||_{\mathcal{L}(X_{NM})} = 1\,, \quad \forall \Delta t \in \mathbb{R}\,. \tag{2.15}$$

Finally, one can now discretize in space the continuous system (2.5) and denote by $\psi_{NM}(t)$ the exact solution of

$$\begin{cases} \partial_t \psi_{NM}^{(1)} = \tilde{G}_{NM}\psi_{NM}^{(1)}\,, \quad \text{on} \quad (0,\varepsilon) \\ \psi_{NM}^{(1)}(t=0) = \psi_{NM}^0 \end{cases}, \quad \begin{cases} \partial_t \psi_{NM}^{(2)} = \tilde{G}_{0,NM}\psi_{NM}^{(2)}\,, \quad \text{on} \quad (\varepsilon,T) \\ \psi_{NM}^{(2)}(t=\varepsilon) = \psi_{NM}^{(1)}(\varepsilon)\,, \end{cases} \tag{2.16}$$

which has the explicit form $\psi_{NM}^{(1)}(t) = \mathcal{G}_{NM}(t)\psi_{NM}^0$ for $t \in [0,\varepsilon]$ and $\psi_{NM}^{(2)}(t) = \mathcal{G}_{0,NM}(t-\varepsilon)\psi_{NM}^{(1)}(\varepsilon)$ for $t \in [\varepsilon, T]$. The initial condition is given by $\psi_{NM}^0 := \mathcal{P}_{NM}(\psi_0)$.
We are now able to apply exactly the same splitting and time-discretization steps to system (2.16) as we did previously to the completely continuous system (2.5). The only difference between (2.16) and (2.5) is that $\tilde{G}_{NM} \in \mathbb{C}^{NM\times NM}$ is a bounded operator, whereas $\tilde{G} : D(G) \subset X \to X$ was unbounded. However, the norm of $\tilde{G}_{NM}$ depends on the spatial

discretization step size and tends to infinity as the latter tends to zero.

Denoting by $\psi_{ij}^n$ the fully numerical solution approximating the exact solution $\psi(t_n, x_i, y_j)$ of (2.5), we get the fully discretized Lie-scheme

$$(L)\ \ \psi^{n+1} = L_{NM}^K(\Delta t)\psi^n := (I - \Delta t \tilde{B}_{NM})^{-1}(I - \Delta t \tilde{A}_{NM})^{-1}\psi^n\,, \tag{2.17}$$

the fully discretized Peaceman-Rachford-scheme

$$(PR)\ \ \psi^{n+1} = P_{NM}^K(\Delta t)\psi^n := (I - \frac{\Delta t}{2}\tilde{B}_{NM})^{-1}(I + \frac{\Delta t}{2}\tilde{A}_{NM})(I - \frac{\Delta t}{2}\tilde{A}_{NM})^{-1}(I + \frac{\Delta t}{2}\tilde{B}_{NM})\psi^n\,, \tag{2.18}$$

and finally the fully discretized Crank-Nicolson scheme

$$(CN)\ \ \psi^{n+1} = C_{NM}^K(\Delta t)\psi^n := (I - \frac{\Delta t}{2}\tilde{G}_{NM})^{-1}(I + \frac{\Delta t}{2}\tilde{G}_{NM})\psi^n\,. \tag{2.19}$$

The starting point for these iterations is $\psi^0 := \mathcal{P}_{NM}\psi_0$. The numerical schemes (2.17), (2.18) and (2.19) are well-defined, due to the properties of the matrices $\tilde{A}_{NM}$, $\tilde{B}_{NM}$ and $\tilde{G}_{NM}$. As usual, the matrix $F_{NM}^K \in \mathbb{C}^{NM\times NM}$ shall stand in the sequel for one of the matrices $L_{NM}^K$, $P_{NM}^K$ or $C_{NM}^K \in \mathbb{C}^{NM\times NM}$. Keep again in mind, that for $n \geq n_0$ the operators $\tilde{B}_{NM}$ and $\tilde{G}_{NM}$ reduce to $\tilde{B}_{0,NM}$ and $\tilde{G}_{0,NM}$. All the notations used in this section are summarized for clarity in Table 1.

| | | |
|---|---|---|
| $\psi(t) := \begin{cases} \mathcal{G}(t)\psi_0\,,\ t\in[0,\varepsilon] \\ \mathcal{G}_0(t-\varepsilon)\psi(\varepsilon)\,,\ t\geq\varepsilon \end{cases}$ | exact sol. of the 2D Schrödinger eq. | (2.5) |
| $\psi_{NM}(t) := \begin{cases} \mathcal{G}_{NM}(t)\psi_{NM}^0\,,\ t\in[0,\varepsilon] \\ \mathcal{G}_{0,NM}(t-\varepsilon)\psi_{NM}(\varepsilon) \end{cases}$ | exact semi-discrete (in space) sol. | (2.16) |
| $\psi_{spl}(t_n) := [\mathcal{F}(\Delta t)]^n\psi_0$<br>$n\Delta t = t_n$ | exact split sol.<br>Lie or Strang split. meth. | (2.9)<br>(2.10)-(2.11) |
| $\psi_{spl}^n := [F^K(\Delta t)]^n\psi_0$ | semi-discrete (in time) split sol.<br>Lie or Peaceman-Rachford split. meth. | (2.12), (2.13) |
| $\psi_{CN}^n := [C^K(\Delta t)]^n\psi_0$ | semi-discrete Crank-Nicolson sol. | (2.8) |
| $\psi^n = [F_{NM}^K(\Delta t)]^n(\mathcal{P}_{NM}\psi_0)$<br>$n\Delta t = t_n$ | numerical sol. (fully discretized sol.)<br>Lie, P.-R., C.-N. | (2.17), (2.18)<br>(2.19) |

TABLE 1. Notations used for the different approximations.

## 3. Numerical analysis

The objective of this section is to analyze the convergence, in particular estimate the errors produced by the three methods proposed in this paper for the numerical resolution of the 2D time-dependent Schrödinger equation (2.5).

Concerning the stability properties of the schemes, it is immediate from (2.15) that the Crank-Nicolson and the Lie schemes are stable, however we observe that for the Peaceman-Rachford scheme, we have only

$$||\psi^{n+1}||_{X_{NM}} = ||P_{NM}^K(\Delta t)\psi^n||_{X_{NM}} \leq ||(I + \frac{\Delta t}{2}\tilde{B}_{NM})\psi^0||_{X_{NM}}\,, \quad \forall n \in \mathbb{N}\,.$$

To show the stability of this PR scheme, let us analyze in detail the (round-off and discretization) error propagation. For this, compare the unperturbed, exact scheme (2.18) with the perturbed one

$$\begin{cases} (I - \frac{\Delta t}{2}\tilde{A}_{NM})\tilde{\psi}^{n+1/2} = (I + \frac{\Delta t}{2}\tilde{B}_{NM})\tilde{\psi}^n + \Delta t\,\delta_{n+1/2}\,, \\ (I - \frac{\Delta t}{2}\tilde{B}_{NM})\tilde{\psi}^{n+1} = (I + \frac{\Delta t}{2}\tilde{A}_{NM})\tilde{\psi}^{n+1/2} + \Delta t\,\delta_{n+1}\,. \end{cases}$$

Here $\delta_n$ denotes the round-off and discretization errors introduced at each step. Denoting now the error by $e^n := \tilde{\psi}^n - \psi^n$, we have the recursive formula

$$\begin{aligned} e^{n+1} &= (I - \tfrac{\Delta t}{2}\tilde{B}_{NM})^{-1}(I + \tfrac{\Delta t}{2}\tilde{A}_{NM})(I - \tfrac{\Delta t}{2}\tilde{A}_{NM})^{-1}(I + \tfrac{\Delta t}{2}\tilde{B}_{NM})\,e^n + \\ &\quad \Delta t(I - \tfrac{\Delta t}{2}\tilde{B}_{NM})^{-1}(I + \tfrac{\Delta t}{2}\tilde{A}_{NM})(I - \tfrac{\Delta t}{2}\tilde{A}_{NM})^{-1}\delta_{n+1/2} + \Delta t(I - \tfrac{\Delta t}{2}\tilde{B}_{NM})^{-1}\delta_{n+1}\,. \end{aligned}$$

Multiplying this equation by $(I + \frac{\Delta t}{2}\tilde{B}_{NM})$ and estimating, we get

$$||(I + \frac{\Delta t}{2}\tilde{B}_{NM})e^{n+1}||_{X_{NM}} \leq ||(I + \frac{\Delta t}{2}\tilde{B}_{NM})e^n||_{X_{NM}} + \Delta t\,||\delta_{n+1/2}||_{X_{NM}} + \Delta t\,||\delta_{n+1}||_{X_{NM}}\,.$$

Taken together, we get

$$||e^n||_{X_{NM}} \leq ||(I + \frac{\Delta t}{2}\tilde{B}_{NM})e^n||_{X_{NM}} \leq ||(I + \frac{\Delta t}{2}\tilde{B}_{NM})e^0||_{X_{NM}} + 2\max_{1\leq i\leq 2n}||\delta_{\frac{1}{2}i}||_{X_{NM}}\,,$$

which shows the stability of the PR scheme with respect to the round-off and discretization errors $\delta_{\frac{1}{2}i}$ as well as initial error, supposing that $(I + \frac{\Delta t}{2}\tilde{B}_{NM})e^0$ remains bounded, independently of the meshes and of $\varepsilon$.

In Section 3.1 we estimate the space-discretization error, between the exact solution $\psi(t)$ and the spatially semi-discretized one $\psi_{NM}(t)$, i.e.

$$\mathcal{E}_x(t) := ||\mathcal{P}_{NM}(\psi(t)) - \psi_{NM}(t)||_{X_{NM}}\,, \quad t \in [0,T]\,.$$

In Section 3.2 we investigate the time discretization error $\mathcal{E}_{CN}^n$ for the Crank-Nicolson scheme and in Section 3.3 the splitting-time discretization error $\mathcal{E}_{spl}^n$, where *spl* stands for one of the two splitting methods $L$ or $PR$, i.e.

$$\mathcal{E}_{CN,spl}^n := ||\psi_{NM}(t_n) - \psi^n||_{X_{NM}}\,, \quad n = 0, \cdots, K\,.$$

Here, as usual, $\psi^n$ stands for the fully discretized solution, obtained from one of the three schemes. The estimate of the global error for $n = 0, \cdots, K$

$$\mathcal{E}^n := ||\mathcal{P}_{NM}\left(\psi(t_n)\right) - \psi^n||_{X_{NM}} \leq ||\mathcal{P}_{NM}\left(\psi(t_n)\right) - \psi_{NM}(t_n)||_{X_{NM}} + ||\psi_{NM}(t_n) - \psi^n||_{X_{NM}}\,,$$

as well as the convergence theorem are given in Section 3.4.
We shall suppose for the rest of this section, that the initial condition $\psi_0$ is sufficiently smooth, for example $\psi_0 \in D(G^3)$, which implies $\psi(t) \in D(G^3)$ for all $t \in [0,T]$.

3.1. **Space discretization.** Let us first estimate the error between the exact solution $\psi(t)$ and the spatially semi-discretized one $\psi_{NM}(t)$ in the time-interval $[0,\varepsilon]$, where we recall that one has

$$\left\{ \begin{array}{l} \partial_t \psi = \tilde{G}\psi\,, \quad \text{on } (0,\varepsilon) \\ \psi(t=0) = \psi_0 \end{array} \right. ; \qquad \left\{ \begin{array}{l} \partial_t \psi_{NM} = \tilde{G}_{NM}\psi_{NM}\,, \quad \text{on } (0,\varepsilon) \\ \psi_{NM}(t=0) = \psi^0_{NM} \end{array} \right. ,$$

with $\psi^0_{NM} = \mathcal{P}_{NM}(\psi_0)$ and $\tilde{G}_{NM} \in \mathbb{C}^{NM\times NM}$ the matrix corresponding to the space discretization of the unbounded operator $\tilde{G}$. Denoting by

$$R_{NM}\psi := \mathcal{P}_{NM}(\tilde{G}\psi) - \tilde{G}_{NM}(\mathcal{P}_{NM}\psi)\,,$$

a simple Taylor expansion yields the estimate

$$||R_{NM}\psi(t)||_{X_{NM}} \leq C\frac{(\Delta x)^2}{\varepsilon}||\partial_x^4\psi(t)||_X + C\frac{(\Delta y)^2}{\delta}||\partial_y^4\psi(t)||_X\,, \quad \forall t\in[0,\varepsilon]\,, \tag{3.20}$$

which is valid also in $[\varepsilon,T]$ if we replace the operators $\tilde{G}$ resp. $\tilde{G}_{NM}$ by $\tilde{G}_0$ resp. $\tilde{G}_{0,NM}$. Applying now the projection operator $\mathcal{P}_{NM}$ to the continuous problem, we get

$$\left\{ \begin{array}{l} \partial_t \mathcal{P}_{NM}(\psi) = \tilde{G}_{NM}\mathcal{P}_{NM}(\psi) + R_{NM}\psi\,, \quad \text{on } (0,\varepsilon)\,, \\ \mathcal{P}_{NM}(\psi(t=0)) = \mathcal{P}_{NM}(\psi_0) = \psi^0_{NM}\,, \end{array} \right.$$

the error function $E_{NM}(t) := \mathcal{P}_{NM}(\psi(t)) - \psi_{NM}(t)$ satisfying thus

$$\left\{ \begin{array}{l} \partial_t E_{NM}(t) = \tilde{G}_{NM}E_{NM}(t) + R_{NM}\psi(t)\,, \quad \text{on } (0,\varepsilon)\,, \\ E_{NM}(t=0) = 0\,. \end{array} \right.$$

By Duhamel's formula we have for $t\in[0,\varepsilon]$

$$E_{NM}(t) = \int_0^t \mathcal{G}_{NM}(t-\tau)R_{NM}\psi(\tau)d\tau\,, \quad ||E_{NM}(t)||_{X_{NM}} \leq t\max_{0\leq\tau\leq t}||R_{NM}\psi(\tau)||_{X_{NM}}\,.$$

Similar computations for the free-motion time-interval $[\varepsilon,T]$ yield

$$\left\{ \begin{array}{l} \partial_t E_{NM}(t) = \tilde{G}_{0,NM}E_{NM}(t) + R_{0,NM}\psi(t)\,, \quad \text{on } (\varepsilon,T)\,, \\ E_{NM}(t=\varepsilon) = \mathcal{P}_{NM}(\psi(\varepsilon)) - \psi_{NM}(\varepsilon)\,, \end{array} \right.$$

implying for $t\in[\varepsilon,T]$

$$E_{NM}(t) = \mathcal{G}_{0,NM}(t-\varepsilon)\left[\mathcal{P}_{NM}(\psi(\varepsilon)) - \psi_{NM}(\varepsilon)\right] + \int_\varepsilon^t \mathcal{G}_{0,NM}(t-\tau)R_{0,NM}\psi(\tau)d\tau\,,$$

and thus

$$\begin{aligned} ||E_{NM}(t)||_{X_{NM}} &\leq ||\mathcal{P}_{NM}(\psi(\varepsilon)) - \psi_{NM}(\varepsilon)||_{X_{NM}} + (t-\varepsilon)\max_{\varepsilon\leq\tau\leq t}||R_{0,NM}\psi(\tau)||_{X_{NM}} \\ &= ||E_{NM}(\varepsilon)||_{X_{NM}} + (t-\varepsilon)\max_{\varepsilon\leq\tau\leq t}||R_{0,NM}\psi(\tau)||_{X_{NM}}\,, \quad \forall t\in[\varepsilon,T]\,. \end{aligned}$$

Let us now analyze in detail these error estimates, in particular let us investigate the terms $||\partial_x^4\psi(t)||_X$ resp. $||\partial_y^4\psi(t)||_X$. For this remark that

$$\begin{cases} \psi(t) = \mathcal{G}(t)\psi_0 = \mathcal{G}_0(t)\psi_0 - \frac{\mathbf{i}}{\varepsilon}\int_0^t \mathcal{G}_0(t-\tau)V\psi(\tau)\,d\tau\,, \quad \forall t\in[0,\varepsilon] \\ \psi(t) = \mathcal{G}_0(t-\varepsilon)\psi(\varepsilon)\,, \quad \forall t\in[\varepsilon,T]\,. \end{cases}$$

The fact that, in the $L^2$-norm the semi-group $\mathcal{G}_0(t)$ commutes with all space derivatives of $\psi$ (see (2.7)) and that $V$ is smooth enough, yields

$$||\partial_x^4\psi(t)||_X \leq C||\psi_0||_{H^4(\Omega)}\,, \quad ||\partial_y^4\psi(t)||_X \leq C||\psi_0||_{H^4(\Omega)}\,, \quad \forall t\in[0,T]\,,$$

and we finally get the estimate

$$\mathcal{E}_x(t) = ||E_{NM}(t)||_{X_{NM}} \leq Ct\left(\frac{(\Delta x)^2}{\varepsilon} + \frac{(\Delta y)^2}{\delta}\right)||\psi_0||_{H^4(\Omega)}\,, \quad \forall t\in[0,T]\,.$$

Remark the $\varepsilon$-dependence of the error, which gives a criterion for the choice of the grid step, much finer in the light-particle coordinate than in the heavy-particle coordinate.

3.2. **Error analysis for the Crank-Nicolson scheme.** Let us now investigate the error produced when discretizing in time the system

$$\begin{cases} \partial_t\psi_{NM}^{(1)} = \tilde{G}_{NM}\psi_{NM}^{(1)}\,, \quad \text{on } (0,\varepsilon) \\ \psi_{NM}^{(1)}(t=0) = \psi_{NM}^0 \end{cases}, \quad \begin{cases} \partial_t\psi_{NM}^{(2)} = \tilde{G}_{0,NM}\psi_{NM}^{(2)}\,, \quad \text{on } (\varepsilon,T)\,, \\ \psi_{NM}^{(2)}(t=\varepsilon) = \psi_{NM}^{(1)}(\varepsilon)\,, \end{cases} \tag{3.21}$$

by means of the Crank-Nicolson scheme, written for $n = 0,\cdots,K$

$$\psi^{n+1} = C_{NM}^K(\Delta t)\,\psi^n = (I - \frac{\Delta t}{2}\tilde{G}_{NM})^{-1}(I + \frac{\Delta t}{2}\tilde{G}_{NM})\,\psi^n\,, \tag{3.22}$$

where for $n \geq n_0$ the operator $\tilde{G}_{NM}$ reduces to $\tilde{G}_{0,NM}$. Regarding first at the time-interval $(0,\varepsilon)$, the error between the exact solution of (3.21), given by $\psi_{NM}(t) = \mathcal{G}_{NM}(t)\psi_{NM}^0$, and the numerical solution $\psi^n$, is

$$\begin{aligned} \psi_{NM}(t_n) - \psi^n &= [\mathcal{G}_{NM}(\Delta t)]^n\psi_{NM}^0 - [C_{NM}^K(\Delta t)]^n\psi_{NM}^0\,, \quad n = 0,\cdots,n_0 \\ &= -\sum_{l=0}^{n-1}[C_{NM}^K(\Delta t)]^{n-l-1}(C_{NM}^K(\Delta t) - \mathcal{G}_{NM}(\Delta t))[\mathcal{G}_{NM}(\Delta t)]^l\psi_{NM}^0\,. \end{aligned} \tag{3.23}$$

A Taylor expansion yields for $l = 0, \cdots, n_0 - 1$

$$(I - \frac{\Delta t}{2}\tilde{G}_{NM})\psi_{NM}(t_{l+1}) = (I + \frac{\Delta t}{2}\tilde{G}_{NM})\psi_{NM}(t_l) + (\Delta t)^3(\tilde{G}_{NM})^3\left(\frac{1}{4}\psi_{NM}(\eta_l) - \frac{1}{6}\psi_{NM}(\xi_l)\right),$$

with $\eta_l,\ \xi_l \in (t_l, t_{l+1})$. Thus

$$||(C^K_{NM}(\Delta t) - \mathcal{G}_{NM}(\Delta t))[\mathcal{G}_{NM}(\Delta t)]^l\psi^0_{NM}||_{X_{NM}} \leq C(\Delta t)^3||\tilde{G}^3_{NM}\psi^0_{NM}||_{X_{NM}},$$

where we used the conservation property $||\tilde{G}^3_{NM}\psi_{NM}(t)||_{X_{NM}} = ||\tilde{G}^3_{NM}\psi^0_{NM}||_{X_{NM}}$ for all $t \in [0, \varepsilon]$. Due to the stability property $||C^K_{NM}(\Delta t)||_{\mathcal{L}(X_{NM})} = 1$, the error estimate is immediately deduced from (3.23)

$$\mathcal{E}^n_{CN} := ||\psi_{NM}(t_n) - \psi^n||_{X_{NM}} \leq C\varepsilon(\Delta t)^2||\tilde{G}^3_{NM}\psi^0_{NM}||_{X_{NM}}, \quad \forall n = 1, \cdots, n_0, \qquad (3.24)$$

where we recall that $n_0\Delta t = \varepsilon$. Similarly we can deduce for the remainder of the interval $[\varepsilon, T]$

$$\begin{aligned} ||\psi_{NM}(t_n) - \psi^n||_{X_{NM}} &\leq ||\left([\mathcal{G}_{0,NM}(\Delta t)]^{n-n_0} - [C^K_{NM}(\Delta t)]^{n-n_0}\right)\psi_{NM}(\varepsilon)||_{X_{NM}} \\ &\quad + |||[C^K_{NM}(\Delta t)]^{n-n_0}(\psi_{NM}(\varepsilon) - \psi^{n_0})||_{X_{NM}}, \quad n \geq n_0 \\ &\leq C(\Delta t)^2||\tilde{G}^3_{0,NM}\psi_{NM}(\varepsilon)||_{X_{NM}} + ||\psi_{NM}(\varepsilon) - \psi^{n_0}||_{X_{NM}}. \end{aligned}$$

In general, $\psi_0$ is independent on $\varepsilon$, implying thus

$$\mathcal{E}^n_{CN} \leq \begin{cases} C\varepsilon(\Delta t)^2||\tilde{G}^3_{NM}\psi^0_{NM}||_{X_{NM}} \leq C\frac{(\Delta t)^2}{\varepsilon^2}, & n \leq n_0 \\ \mathcal{E}^{n_0}_{CN} + C(\Delta t)^2||\tilde{G}^3_{0,NM}\psi_{NM}(\varepsilon)||_{X_{NM}} \leq C\frac{(\Delta t)^2}{\varepsilon^3}, & n > n_0, \end{cases}$$

which shows a drastic dependence of the error on the small parameter $\varepsilon$, especially for $n > n_0$. In other words, for a desired precision of magnitude $\tau$ at the final time $T$, we have to choose a time step $\Delta t < (\tau\varepsilon^3)^{1/2}$ which is very restrictive and unfeasible from a numerical point of view if $0 < \varepsilon \ll 1$. This strong $\varepsilon$-dependence of the time discretization error comes from the fact, that while the light particle dynamics is rapid, we are interested in computing the solution up to the final time $T$, which takes a large value as compared to the characteristic light-particle time.

In Figure 2 (left), the author plotted the condition number of the matrix $I - \frac{\Delta t}{2}\tilde{G}_{NM}$, which is the matrix of the linear system to be solved at each time step $t_n$ to get $\psi^n$ (see (3.22)). Notice particularly the $1/\varepsilon$-dependence of this condition number, which underlines the fact that the problem becomes ill-posed (for fixed grids) in the limit $\varepsilon \to 0$. In Figure 2 (right), the author plotted four curves obtained by the Crank-Nicolson scheme and representing for a fixed grid ($\Delta t$, $\Delta x$, $\Delta y$) and four different masses $\varepsilon$, the heavy particle density function $\rho_H(\overline{t}, y)$, defined in the introduction by (1.2) and taken at instant $\overline{t} := \frac{y_0\delta}{P_H}$, corresponding to the moment when the two heavy-particle wave-packets completely overlap and create

an interference pattern. The disappearance of the interference fringes due to the heavy-light particle collision is the so-called decoherence effect, describing the transition from the quantum to the classical world.
Let us remark here that for different $\varepsilon$-values, the solutions $\psi^\varepsilon$ are different. However it is shown in [2, 3] that the probability density $\rho_H^\varepsilon$ tends in the limit $\varepsilon \to 0$ towards an asymptotic limit function. In the figures illustrated here, the asymptotic regime seems to be attained for $\varepsilon \in [3 * 10^{-3}, 6 * 10^{-3}]$. However, for smaller $\varepsilon$-values, the numerical errors take over, and no deductions can be made.

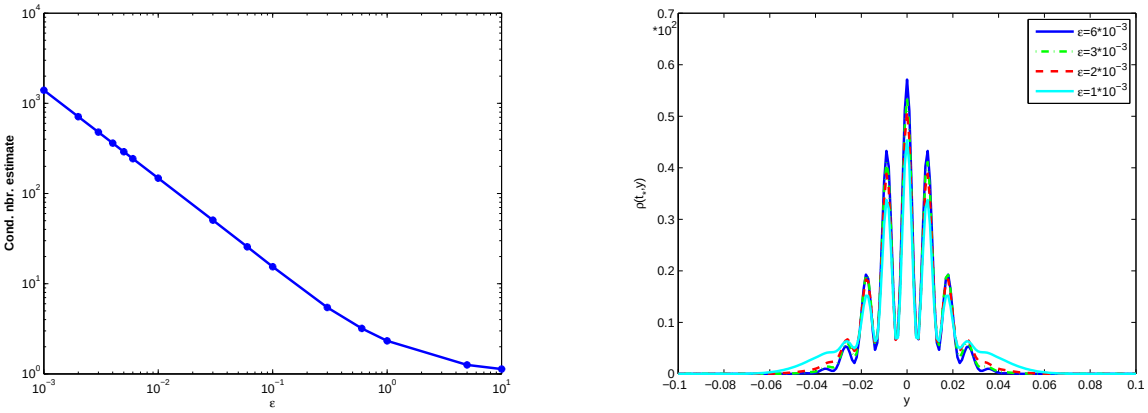


FIGURE 2. Left: Condition number (in $log - log$ scale) for the CN scheme with respect to $\varepsilon$. Right: Heavy particle density, obtained with the CN-scheme for different masses $\varepsilon$. The time-space grid is fixed in both figures.

3.3. **Error analysis for the splitting schemes.** The purpose of this subsection is to estimate the error between the spatially semi-discretized solution $\psi_{NM}(t)$ and the fully numerical split solution $\psi^n$. Let us consider first the interaction interval $[0, \varepsilon]$, *i.e.* $n \leq n_0$, and study

$$\mathcal{E}_{spl}^n = ||\psi_{NM}(t_n) - \psi^n||_{X_{NM}} = ||[\mathcal{G}_{NM}(\Delta t)]^n \psi_{NM}^0 - [F_{NM}^K(\Delta t)]^n \psi_{NM}^0||_{X_{NM}} ,$$

where the split solution is obtained either by the Lie-splitting method (2.17) or the Peaceman-Rachford split method (2.18).

Th achieve this, we define the bounded operators $\lambda_j \in \mathcal{L}(X_{NM})$ [12]

$$\lambda_0 := \mathcal{G}_{NM}(\Delta t) , \quad \lambda_j := \frac{1}{(\Delta t)^j} \int_0^{\Delta t} \mathcal{G}_{NM}(\Delta t - \tau) \frac{\tau^{j-1}}{(j-1)!} \, d\tau , \quad \forall j \geq 1 .$$

These operators satisfy $||\lambda_j||_{\mathcal{L}(X_{NM})} \leq \frac{1}{j!} \leq 1$ and the recurrence relation

$$\lambda_j = \frac{1}{j!} I + (\Delta t)\tilde{G}_{NM}\lambda_{j+1}\,, \qquad j \geq 0\,, \tag{3.25}$$

which yields in particular

$$I - \lambda_0 = -(\Delta t)\tilde{G}_{NM}\lambda_1\,, \quad \lambda_0 - \lambda_1 = (\Delta t)\tilde{G}_{NM}(\lambda_1 - \lambda_2)\,,$$
$$\frac{1}{2}\lambda_1 - \lambda_2 = (\Delta t)\tilde{G}_{NM}(\frac{1}{2}\lambda_2 - \lambda_3)\,.$$

Formula (3.25) is immediate by a partial integration and the fact that

$$\frac{d}{d\tau}\left[\mathcal{G}_{NM}(\Delta t - \tau)u\right] = -\tilde{G}_{NM}\mathcal{G}_{NM}(\Delta t - \tau)u\,, \quad \forall u \in D(G)\,.$$

Similar to the Crank-Nicolson case, we use the telescopic formula

$$\begin{aligned}\psi^n - \psi_{NM}(t_n) &= [F^K_{NM}(\Delta t)]^n\psi^0_{NM} - [\mathcal{G}_{NM}(\Delta t)]^n\psi^0_{NM}\,, \quad n \leq n_0\\ &= \sum_{l=0}^{n-1}[F^K_{NM}(\Delta t)]^{n-l-1}\left(F^K_{NM}(\Delta t) - \mathcal{G}_{NM}(\Delta t)\right)[\mathcal{G}_{NM}(\Delta t)]^l\,\psi^0_{NM}\,.\end{aligned}$$

In the Lie splitting case, where

$$F^K_{NM}(\Delta t) = (I - \Delta t\tilde{B}_{NM})^{-1}(I - \Delta t\tilde{A}_{NM})^{-1}\,,$$

we can rewrite the operator $F^K_{NM}(\Delta t) - \mathcal{G}_{NM}(\Delta t)$ as follows

$$\begin{aligned}F^K_{NM}(\Delta t) - \mathcal{G}_{NM}(\Delta t) &= F^K_{NM}(\Delta t)\left[I - (I - \Delta t\tilde{A}_{NM})(I - \Delta t\tilde{B}_{NM})\mathcal{G}_{NM}(\Delta t)\right]\\ &= F^K_{NM}(\Delta t)\left[I - \mathcal{G}_{NM}(\Delta t) + (\Delta t)\tilde{G}_{NM}\mathcal{G}_{NM}(\Delta t) - (\Delta t)^2\tilde{A}_{NM}\tilde{B}_{NM}\mathcal{G}_{NM}(\Delta t)\right]\\ &= F^K_{NM}(\Delta t)\left[(\Delta t)^2\tilde{G}^2_{NM}(\lambda_1 - \lambda_2) - (\Delta t)^2\tilde{A}_{NM}\tilde{B}_{NM}\mathcal{G}_{NM}(\Delta t)\right]\,.\end{aligned}$$

This yields for $n \leq n_0$

$$\begin{aligned}\left([F^K_{NM}(\Delta t)]^n - [\mathcal{G}_{NM}(\Delta t)]^n\right)\psi^0_{NM} = (\Delta t)^2\sum_{l=0}^{n-1}[F^K_{NM}(\Delta t)]^{n-l}\Big((\lambda_1 - \lambda_2)[\mathcal{G}_{NM}(\Delta t)]^l\tilde{G}^2_{NM}\\ -\tilde{A}_{NM}\tilde{B}_{NM}[\mathcal{G}_{NM}(\Delta t)]^{l+1}\Big)\psi^0_{NM}\,,\end{aligned}$$

which gives, due to the contractivity of $F^K_{NM}(\Delta t)$ and the fact, that $n_0\Delta t = \varepsilon$

$$\mathcal{E}^n_L \leq C\varepsilon\Delta t\left(||\tilde{G}^2_{NM}\psi^0_{NM}||_{X_{NM}} + ||\tilde{A}_{NM}\tilde{B}_{NM}\,\psi_{NM}(t_{l+1})||_{X_{NM}}\right) \leq C\frac{\Delta t}{\varepsilon}\,, \quad n = 1, \cdots, n_0\,.$$

For the Peaceman-Rachford splitting method

$$F^K_{NM}(\Delta t) = (I - \frac{\Delta t}{2}\tilde{B}_{NM})^{-1}(I + \frac{\Delta t}{2}\tilde{A}_{NM})(I - \frac{\Delta t}{2}\tilde{A}_{NM})^{-1}(I + \frac{\Delta t}{2}\tilde{B}_{NM})\,,$$

we have

$$F^K_{NM}(\Delta t) - \mathcal{G}_{NM}(\Delta t) =$$

$$(I - \tfrac{\Delta t}{2}\tilde{B}_{NM})^{-1}(I - \tfrac{\Delta t}{2}\tilde{A}_{NM})^{-1}\Big[(I + \tfrac{\Delta t}{2}\tilde{A}_{NM})(I + \tfrac{\Delta t}{2}\tilde{B}_{NM}) - (I - \tfrac{\Delta t}{2}\tilde{A}_{NM})(I - \tfrac{\Delta t}{2}\tilde{B}_{NM})\lambda_0\Big]$$

$$(I - \tfrac{\Delta t}{2}\tilde{B}_{NM})^{-1}(I - \tfrac{\Delta t}{2}\tilde{A}_{NM})^{-1}\left[I - \lambda_0 + \tfrac{\Delta t}{2}\tilde{G}_{NM}(I + \lambda_0) - \tfrac{(\Delta t)^3}{4}\tilde{A}_{NM}\tilde{B}_{NM}\tilde{G}_{NM}\lambda_1\right]$$

$$(I - \tfrac{\Delta t}{2}\tilde{B}_{NM})^{-1}(I - \tfrac{\Delta t}{2}\tilde{A}_{NM})^{-1}\left[(\Delta t)^3\tilde{G}^3_{NM}(\tfrac{\lambda_2}{2} - \lambda_3) - \tfrac{(\Delta t)^3}{4}\tilde{A}_{NM}\tilde{B}_{NM}\tilde{G}_{NM}\lambda_1\right]$$

Thus, one deduces

$$[F^K_{NM}(\Delta t)]^n\psi^0_{NM} - [\mathcal{G}_{NM}(\Delta t)]^n\psi^0_{NM} =$$

$$(\Delta t)^3\sum_{l=0}^{n-1}[F^K_{NM}(\Delta t)]^{n-l-1}(I - \frac{\Delta t}{2}\tilde{B}_{NM})^{-1}(I - \frac{\Delta t}{2}\tilde{A}_{NM})^{-1}(\frac{\lambda_2}{2} - \lambda_3)[\mathcal{G}_{NM}(\Delta t)]^l\tilde{G}^3_{NM}\psi^0_{NM}$$

$$-\frac{(\Delta t)^3}{4}\sum_{l=0}^{n-1}[F^K_{NM}(\Delta t)]^{n-l-1}(I - \frac{\Delta t}{2}\tilde{B}_{NM})^{-1}(I - \frac{\Delta t}{2}\tilde{A}_{NM})^{-1}\tilde{A}_{NM}\tilde{B}_{NM}\lambda_1[\mathcal{G}_{NM}(\Delta t)]^l\tilde{G}_{NM}\psi^0_{NM}\,.$$

Recalling that $||(I + \frac{\Delta t}{2}\tilde{F}_{NM})(I - \frac{\Delta t}{2}\tilde{F}_{NM})^{-1}||_{\mathcal{L}(X_{NM})} = 1$, one can show that

$$||[F^K_{NM}(\Delta t)]^j(I - \frac{\Delta t}{2}\tilde{B}_{NM})^{-1}v||_{X_{NM}} \leq ||v||_{X_{NM}}\,, \quad \forall v \in X_{NM}\,, \quad \forall j \geq 0\,,$$

implying for $n \leq n_0$

$$\mathcal{E}^n_{PR} \leq C\varepsilon(\Delta t)^2\left(||\tilde{G}^3_{NM}\psi^0_{NM}||_{X_{NM}} + ||\tilde{A}_{NM}\tilde{B}_{NM}\tilde{G}_{NM}\lambda_1\psi_{NM}(t_l)||_{X_{NM}}\right) \leq C\frac{(\Delta t)^2}{\varepsilon^2}\,. \tag{3.26}$$

Note that replacing $\tilde{A}_{NM}$ by zero and $\tilde{B}_{NM}$ by $\tilde{G}_{NM}$, the Peaceman-Rachford scheme transforms into the Crank-Nicolson scheme, and the two error estimates (3.24) and (3.26) coincide.

To consider now the free-motion error estimate in $[\varepsilon, T]$, we have only to replace the operators $\tilde{G}_{NM}$ resp. $\tilde{B}_{NM}$ by $\tilde{G}_{0,NM}$ resp. $\tilde{B}_{0,NM}$ in the previous computations and to observe that

$$\mathcal{E}^n_{spl} \leq ||\psi^{n_0} - \psi_{NM}(\varepsilon)||_{X_{NM}} + ||\left([F^K_{0,NM}(\Delta t)]^{n-n_0} - [\mathcal{G}_{0,NM}(\Delta t)]^{n-n_0}\right)\psi^{n_0}_{NM}||_{X_{NM}}\,,$$

to get for $n \geq n_0$

$$\mathcal{E}^n_L \leq \mathcal{E}^{n_0}_L + C\Delta t\left(||\tilde{G}^2_{0,NM}\psi^{n_0}_{NM}||_{X_{NM}} + ||\tilde{A}_{NM}\tilde{B}_{0,NM}\,\psi^{n_0}_{NM}||_{X_{NM}}\right) \leq C\frac{\Delta t}{\varepsilon^2}\,.$$

$$\mathcal{E}^n_{PR} \leq \mathcal{E}^{n_0}_{PR} + C(\Delta t)^2\left(||\tilde{G}^3_{0,NM}\psi^{n_0}_{NM}||_{X_{NM}} + ||\tilde{A}_{NM}\tilde{B}_{0,NM}\tilde{G}_{0,NM}\psi^{n_0}_{NM}||_{X_{NM}}\right) \leq C\frac{(\Delta t)^2}{\varepsilon^3}\,.$$

3.4. **Convergence results.** We summarize in this subsection, under the form of a convergence theorem, the error estimates deduced in the last subsections and interpret the results.

**Theorem 3.1.** *The three numerical schemes used in this paper for the resolution of the 2D Schrödinger equation (2.5) are convergent, in particular one has:*
*There exists a constant $C > 0$, depending only on the initial condition and the potential $V$, such that the unconditionally stable Lie-scheme (2.17) satisfies the error-estimate*

$$||\mathcal{P}_{NM}\left(\psi(t_n)\right) - \psi^n||_{X_{NM}} \leq Ct_n \left( \frac{\Delta t}{\varepsilon^2} + \left( \frac{(\Delta x)^2}{\varepsilon} + \frac{(\Delta y)^2}{\delta} \right) ||\psi_0||_{H^4(\Omega)} \right), \tag{3.27}$$

*which means it is first order in time and second order in space. The unconditionally stable Crank-Nicolson (2.19) and Peaceman-Rachford (2.18) schemes are second order in space and time, i.e.*

$$||\mathcal{P}_{NM}\left(\psi(t_n)\right) - \psi^n||_{X_{NM}} \leq Ct_n \left( \frac{(\Delta t)^2}{\varepsilon^3} + \left( \frac{(\Delta x)^2}{\varepsilon} + \frac{(\Delta y)^2}{\delta} \right) ||\psi_0||_{H^4(\Omega)} \right). \tag{3.28}$$

The error estimates (3.27)-(3.28) state that the grid has to be adapted with respect to the $\varepsilon$-values in order to remain accurate. This can be seen in Figure 3, where the author plotted the heavy-particle density $\rho_H(\overline{t}, y)$ (at overlap time $\overline{t}$), obtained on a fixed grid via the different methods and three different $\varepsilon$-values. One can observe that for a fixed grid and diminishing $\varepsilon$-values, the methods become inaccurate one after the other. The PR-scheme seems to be, for small $\varepsilon$-values, the most accurate one, even if from estimate (3.28) there seems to be no difference with the CN-scheme. However, we have to keep in mind that in Figure 3 are plotted the heavy-particle density functions, which evolve on a slow time-scale. It is therefore necessary to make a more detailed error study, decoupling the light and the heavy dynamics in order to understand why the PR-scheme is the most performant one when computing the heavy-particle density function. As mentioned in section 3.2, it is this heavy-particle density-function which is interesting for the decoherence effect.
The same behavior can be observed in Figure 4, where we compared in the free motion case $V \equiv 0$ the numerical solutions, obtained via the three methods, with the exact solution. Plotted is the $L^2$-absolute error for several $\varepsilon$-values. Remark that the error gets larger in the small $\varepsilon$-regime, there where we can single out the decoherence effect from other effects, like deformation for example. Again the Peaceman-Rachford scheme seems to be most powerful method. Is is this PR-scheme which is used in the more physical paper [5] for the detailed study of this decoherence effect.
In Table 2 the performances of the three methods are compared with respect to simulation time and precision.

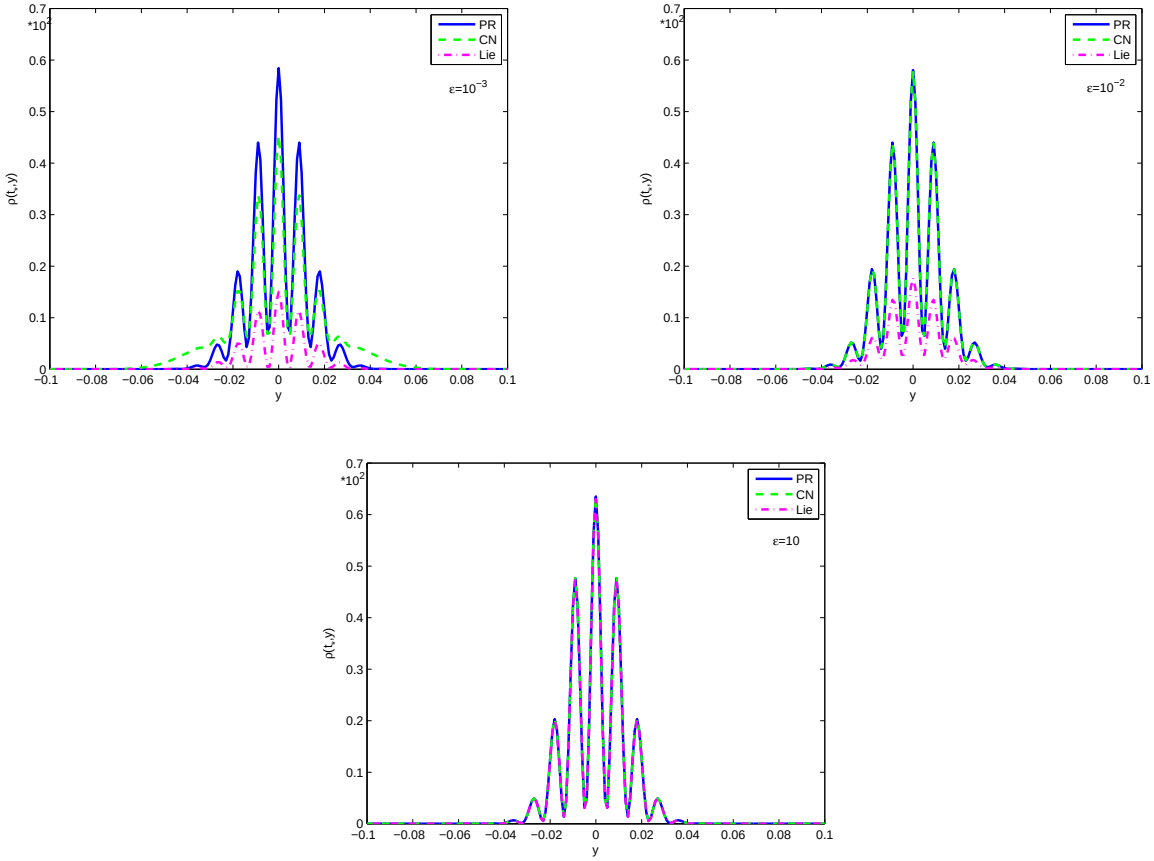


FIGURE 3. Comparison of the heavy-particle density $\rho_H(\bar{t}, y)$, obtained with the methods $PR$, $CN$ resp. $L$ for three different masses $\varepsilon$.

| Method | Rel. $L^2$-error with resp. to ref. sol. $\varepsilon = 10^{-3}$ ; $10^{-2}$ ; 10 | grid | time |
|---|---|---|---|
| Lie | 0.75 ; 0.69 ; 0.022 | $N_x = N_y = 201$ $N_t = 24 * 10^4$ | 2h 10min |
| Crank-Nicolson | 0.24 ; 0.033 ; 0.023 | $N_x = N_y = 201$ $N_t = 24 * 10^3$ | 2h 2min |
| Peaceman-Rachford | 0.038 ; 0.028 ; 0.023 | $N_x = N_y = 201$ $N_t = 24 * 10^3$ | 18 min |

TABLE 2. Performance comparison of the three schemes, corresponding to the three $\varepsilon$-values of the plots in Figure 3.

What we would like to observe is that it is quiet natural to have so drastic $\varepsilon$-dependent error-estimates, as we are computing up to a large final time $T$ the two-body dynamics, the light-particle evolution being rather rapid (dispersion of the order $1/\varepsilon$) and thus demanding a fine time-mesh in order to catch the rapid time-evolutions.
In order to avoid these problems, related to the small $\varepsilon$-values (problems which imply the choice of rather fine time and space grids, leading to long simulations times and large memory savings) one can propose to try to separate the two scales, the rapid light-particle evolution and the slow heavy-particle dynamics, solving them separately. See for example [18].
A performant scheme, based somehow also on the separation of the two dynamics, will be proposed in [4] and is briefly sketched in the next section. The main idea is to try to find a model for solving only the heavy-particle dynamics after the interaction, i.e. for $t > \varepsilon$, without taking care of the light-particle dynamics. Indeed, the rapid light-particle dynamics is (after interaction) of no more interest for the further evolution and its unnecessary computation can be skipped.

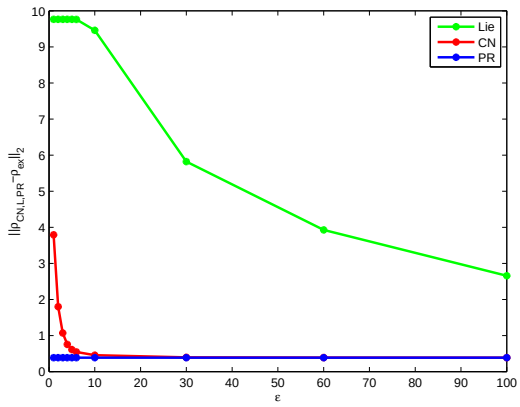


FIGURE 4. Absolute $L^2$-error between the three schemes and the exact solution in the $V \equiv 0$ case.

## 4. Multi-scale resolution method

The sever $\varepsilon$-dependent error estimates of Theorem 3.1 pushes us to search for more efficient schemes for the resolution of the 2D Schrödinger equation (2.5), taking into account or even exploiting the multi-scale nature of the problem. In this section the author shall briefly outline the main ideas of a performant multi-scale scheme for the present problem. The advantages of this new scheme are rather compelling, such that we shall perform a

more detailed mathematical and numerical study in the future work [4].

The heavy-light particle interaction takes place during the short time interval $[0, \varepsilon]$, whereas after the collision, during $[\varepsilon, T]$, the two-particle dynamics becomes free ($V \equiv 0$). Starting from the initial condition $\psi_0$, the idea is to treat differently the two distinct time-periods, in other words the first interaction-time interval $[0, T_\varepsilon]$ and the second free-motion time-interval $[\varepsilon, T]$. As suggested by the asymptotic behavior of the wave-function $\psi$ in the limit $0 < \varepsilon << 1$ (see [1–3]), the two-body dynamics can be approximated as follows (Joos-Zeh approximation): For small mass ratios the dynamics of the heavy particle in presence of the light one can be described by the free Hamiltonian, the interaction with the light particle being expressed in an adequate modification of the heavy-particle initial condition. Let us explain in some more details this approximation.

In the first part of our evolution (corresponding to the interaction evolution), we shall consider that the heavy particle is stationary, as the interaction (collision) is of very short duration $\sim \varepsilon$ (quasi instantaneous). Only the light particle is moving, taking with it all interaction information. Thus we are led to solve for each fixed $y \in \Omega_y$, the 1D time-dependent Schrödinger equation, to get $\psi^I(t, \cdot, y)$ (I: interaction)

$$\begin{cases} \mathbf{i}\partial_t \psi^I = -\frac{1}{\epsilon}\Delta_x \psi^I + \frac{1}{\varepsilon} V(|x-y|)\ \psi^I\,, \quad \text{for} \quad (x,y) \in \Omega\,,\ \ t \in (0,\varepsilon) \\ \partial_x \psi^I(t,x,y) = 0 \quad \text{on} \quad \partial\Omega_x \times \Omega_y\,, \\ \psi^I(0,x,y) = \psi_0(x,y)\,, \quad \text{for} \quad (x,y) \in \Omega\,. \end{cases} \tag{4.29}$$

In the second part of our evolution (corresponding to the free-motion), after the light-heavy particle interaction, we suppose that the light particle does not move any more, and only the heavy particle is evolving. Of course the assumption of a frozen light particle is false in the two-body dynamics and the computed two-body solution will be very different from the physical real two-body solution. However, as we will see in [4], after the interruption of the interaction, the heavy-particle density does not depend any more on the dynamics of the light particle. In this case, it is much simpler, from a numerical point of view, to consider the frozen case. Thus, we shall solve for each fixed $x \in \Omega_x$ the 1D time-dependent Schrödinger equation, to get $\psi^F(t, x, \cdot)$ (F: free)

$$\begin{cases} \mathbf{i}\partial_t \psi^F = -\frac{1}{\delta}\Delta_y \psi^F\,, \quad \text{for} \quad (x,y) \in \Omega\,,\ \ t \in (\varepsilon, T) \\ \partial_y \psi^F(t,x,y) = 0 \quad \text{on} \quad \Omega_x \times \partial\Omega_y \\ \psi^F(\varepsilon,x,y) = \psi^I(\varepsilon,x,y)\,, \quad \text{for} \quad (x,y) \in \Omega\,. \end{cases} \tag{4.30}$$

A rigorous justification, in particular the study of the errors we are doing at each step in the approximation, when solving (4.29)-(4.30) instead of (1.1) will be the aim of [4]. With

this new multi-resolution scheme it will be also possible to investigate the effect of several collisions on the decoherence.

## 5. Conclusion

The numerical study performed in the present paper and concerning three numerical schemes for the resolution of the two-body time-dependent Schrödinger equation indicates that the results obtained in the previous paper [5] are precise for sufficiently fine time and space grids. However, due to the drastic $\varepsilon$-dependence of the errors, the choice of rather fine time and space grids implies very high computational times and memory savings, which is rapidly unfeasible from a computational point of view. Based on these results, a new, very efficient numerical scheme, will be proposed in the forthcoming paper [4]. This new method will separate the two dynamics, the rapid light particle evolution and the slow heavy particle dynamics, and will treat them separately. It shall combine asymptotic methods with splitting methods.

**Acknowledgments.** The author would like to thank Franck Boyer, Thierry Gallouët and Maxime Hauray for their helpful advices and discussions. This work has been supported by the GREFI-MEFI (Groupement De Recherche Européen Franco-Italien) and the ANR QUATRAIN (Quantum transport in nanostructures).
A warm and special thank goes to Naoufel Ben Abdallah, for all he has done for me.

## References

[1] R. Adami, L. Erdős, *Rate of decoherence for an electron weakly coupled to a phonon gas*, J. Stat. Phys. **132** (2008), no. 2, 301–328.
[2] R. Adami, R. Figari, D. Finco, A. Teta, *On the asymptotic behaviour of a quantum two-body system in the small mass ratio limit*, J. Phys. A: Math. Gen., **37** (2004), 7567–7580.
[3] R. Adami, R. Figari, D. Finco, A. Teta, *On the asymptotic dynamics of a quantum system composed by heavy and light particles*, Comm. Math. Phys. **268** (2006), no. 3, 819–852.
[4] R. Adami, M. Hauray, C. Negulescu, *Accelerate and precise numerical resolution of the anisotropic two-body Schrödinger equation. Application to decoherence.*, in preparation.
[5] R. Adami, C. Negulescu, *A numerical model for the study of quantum decoherence*, in preparation.
[6] W. Bao, S. Jin, P.A. Markowich, *Numerical study of time-splitting spectral discretizations of nonlinear Schrodinger equations in the semi-classical regimes* SIAM J. Sci. Comput. **25** (2003), no. 1, 27–64.
[7] A. Batkai, P. Csomos, G. Nickel, *Operator splittings and spatial approximations for evolution equations*, J. of Evolution Equations **9** (2009), no. 3, 613–636.
[8] S. Descombes, M. Thalhammer, *High-order exponential operator splitting methods for evolutionary problems. A local error expansion and applications to the linear Schrödinger equations in the semi-classical regime*, preprint.
[9] G. Dujardin, E. Faou, *Normal form and long time analysis of splitting schemes for the linear Schrdinger equation with small potential* Numer. Math. **106** (2007), no. 2, 223–262.

[10] L. Gauckler, C. Lubich, *Splitting integrators for nonlinear Schrdinger equations over long times*, Found. Comput. Math. **10** (2010), no. 3, 275 302.
[11] G. Dujardin, E. Faou, *Long time behavior of splitting methods applied to the linear Schrdinger equation*, C. R. Acad. Sci. Paris, Sér. I. **344** (2007), 89–92.
[12] E. Hansen, A. Ostermann, *Dimension splitting for evolution equations*, Numer. Math. **108** (2008), 557–570.
[13] R. Horn, C. R. Johnson, *Matrix Analysis*, Cambridge U.P., 1985.
[14] W.H. Hundsdorfer, J.G. Verwer, *Stability and convergence of the Peaceman-Rachford ADI method for initial-boundary value problems*, Math. of Comp. **53** (1989), no. 187, 81–101.
[15] T. Jahnke, Ch. Lubich, *Error bounds for exponential operator splittings*, BIT **40** (2000), 735 -744.
[16] A. Pazy, *Semigroups of linear operators and applications to partial differential equations*, Springer-Verlag, New-York, 1983.
[17] M. Schatzman, *Stability of the Peaceman-Rachford approximation*, J. Functional Analysis **162** (1999), 219–255.
[18] B. Sportisse, *An analysis of operator splitting techniques in the stiff case*, Journal of Computational Physics **161** (2000), 140–168.

CMI/LATP (UMR 6632), Université de Provence, 39 rue Joliot Curie, 13453 Marseille Cedex 13, France

*E-mail address*: claudia.negulescu@cmi.univ-mrs.fr